

## Synthesis, Characterization, and Application of Dendrimer Modified Magnetite Nanoparticles as Antimicrobial Agent

Samia M. El-Sigeny<sup>1</sup>, Manal F. Abou Taleb<sup>2</sup>

<sup>1</sup>Department of Chemistry, Faculty of Science, Kafr El-Sheikh University, 33516 Kafr El - Sheikh, Egypt

<sup>2</sup>Polymer Chemistry Department, National Center for Radiation Research and Technology, P. O. Box No. 29, Nasr city, Cairo, 11731 Egypt  
[shelsigeny@yahoo.com.hk](mailto:shelsigeny@yahoo.com.hk)

**Abstract:** Synthesis and characterization of different generations ( $G_0$ – $G_5$ ) of polyamidoamine (PAMAM) dendrimer-coated  $Fe_3O_4$  nanoparticles using ethyl acrylate and 1,3-propane diamine have been reported in this study. Superparamagnetic iron oxide  $Fe_3O_4$  nanoparticles were synthesized by co-precipitation method and modified with tris(hydroxymethylamino) methane hydrochloride for dendrimer coating. Physical characterization of the newly prepared PAMAM dendrimer-coated  $Fe_3O_4$  nanocomposite have been carried out by using infrared spectrophotometer (IR), Transmission electron microscope (TEM), steady-state spectrophotometer (UV-Vis), thermogravimetric analysis (TGA), and X-ray diffraction. TEM images demonstrated that the PAMAM dendrimer-coated nanocomposite have monodisperse of 7.3–6.3 nm. The antimicrobial activity of the PAMAM dendrimer-coated  $Fe_3O_4$  nanoparticles and  $Fe_3O_4$  nanoparticles were tested against various microorganisms *Staphylococcus aureus* (+ve) Gram and (-ve) *Escherichia coli* bacteria. In general, the PAMAM dendrimer-coated  $Fe_3O_4$  nanoparticles showed good antimicrobial activity.

[Samia M. El-Sigeny, Manal F. Abou Taleb. **Synthesis, Characterization, and Application of Dendrimer Modified Magnetite Nanoparticles as Antimicrobial Agent.** *Life Sci J* 2015;12(6):161-170]. (ISSN:1097-8135). <http://www.lifesciencesite.com>. 21

**Keywords:** Dendrimer; Magnetic nanoparticles; Iron oxide; Antimicrobial activity.

### 1. Introduction

Dendritic polymers are synthesized using a stepwise repetitive reaction, (Tomalia et. al. 1990) with nearly perfect hyperbranched topology radiating from a central core and grown generation by generation. The synthetic procedures developed for dendrimer preparation permit nearly complete control over the critical molecular design parameters (e.g., size, shape, surface interior chemistry, flexibility and topology), which make them useful in the practical applications (El-Khouly et. al. 2008; El-Khouly et. al. 2009). Synthetic techniques proved effective in generating macromolecules with a unique combination of properties include the starburst divergent strategy, the convergent growth strategy, and the self-assembly strategy. Dendrimers are macromolecules with highly branched three-dimensional architecture and have some unique properties because of their globular shape and the presence of free-void volume in their internal cavities. Due to the free-void volume located within the interior structure of the dendrimer. It can encapsulate guest molecules in its macromolecular interior, thus coating the nanoparticles and potentially preventing them from further oxidation and aggregation (Gao 2005).

Iron oxide magnetic nanoparticles are used in important bio applications (Mornet et.al. 2004; Huh et.al.2005 ), including magnetic bioseparation and detection of entities (cell, protein, nucleic acids,

enzymes, bacterial, etc.) clinic diagnosis and therapy such as MRI (magnetic resonance image) and MFH (magnetic fluid hyperthermia) (Gupta and Gupta 2005; Ito et.al. 2004), targeted drug delivery and biological labels (Jain et.al. 2005).

The magnetic iron oxide NPs became the strong candidates, and the application of small iron oxide NPs in vitro diagnostics has been practiced for nearly half a century (Gupta and Gupta 2005; Ito et.al. 2004). Magnetics iron oxide have large surface and have high chemical activity. The size effect and surface chemistry play a major role in the biological applications.

To control the surface properties of iron oxide nanoparticles coating is applied with a biocompatible polymer during or after the synthesis process (Mornet 2005; Chan 2006; Chan et.al. 2006) to overcome the toxicity at high – level accumulation in the target tissue, the iron oxide nanoparticles (IONPs) may be subjected to further functionalization using bioactive material.

The polyamidoamine (PMAM) dendrimer - modified with iron oxide magnetic nanoparticles (MNPs) have the internal cavities makes them suitable for application in gene therapy and cancer therapy. The dendrimers-modified (MNPs) are good non-viral synthetic vectors and have the advantages of safety, and simplicity of use. They are synthesized through different cycle or "generations" by adding branched monomers that react with the functional groups of the

core such as iron-oxide nanoparticles after which the free end groups of monomers can further react. Thus, the number of terminal groups will increase of each generation of the synthesis (Sevenson and Tomalia 2005; Duncan and Izzo 2005).

Furthermore, with increasing microbial organisms resistant to various antibiotics and uncertainties in health care costs, the emergence of more cost effective new methodologies to produce nanosized particles with specific physical and chemical functionalities and with limited or no resistance has piqued the interest of scientists around the globe (Pankhurst et.al. 2009; Kim et.al. 2007; Theivasanthi and Alagar, 2011). That is, the development of more cost efficient synthetic methodologies with the capability of producing nanoparticles with highly controllable sizes and chemical functionalities will increase the possibilities of developing new types of nanostructures with well-designed (or even specific) functional surfaces or architectures that can be used in the biomedical industry as antimicrobial agents. The antimicrobial activity exhibited by nanoparticles has been attributed to their relatively smaller sizes and high amount of surface-area-to-volume ratio that allows nanoparticles to interact closely with membranes of viruses, fungi, or bacteria.

Toward this target, we describe herein the first report of direct formation of a cascading polyamino amine PAMAM dendrimer on the surface of tris (hydroxymethyl) amino methane hydrochloride modified with iron oxide magnetite nanoparticles and study the physical – chemical properties. TEM, FT-IR, TGA, Zeta potential analysis, and UV-Vis spectroscopy were used to characterize the structure composition. Thus, in this study the biological activity of the nanoparticles against (+ve) Gram *staphylococcus auries*, and (-ve) Gram *scherichia coli* bacteria is investigated.

## 2. Material and methods

### Materials

Ferric chloride hexahydrate ( $\text{FeCl}_3 \cdot 6\text{H}_2\text{O}$ ), ferrous chloride tetrahydrate ( $\text{FeCl}_2 \cdot 4\text{H}_2\text{O}$ ) and ammonium hydroxide (25 wt%) were purchased from Fluka. Ethylacrylate and 1,3- propane diamine were obtained from Sigma-Aldrich. Tris(hydroxymethyl)amino methane hydrochloride was purchased from Sigma (USA). All chemicals were of analytical grade and used as received.

### Instrumentation

Absorbance measurement was carried out on UNICAM UV-Vis Spectrometer 1000 Model spectrophotometer. Fourier transform infrared (FTIR) spectra were obtained in the transmission mode using Mattson 1000, Unicam infrared spectrophotometer Cambridge, England. The spectra were covered the

infrared region 4000 to  $400\text{ cm}^{-1}$  using KBr pellets. The XRD analysis was performed at room temperature using XD-DI Series, Shimadzu apparatus using nickel-filtered and Cu-K $\alpha$  target. The zeta potential measurement was carried out on Zeta potential analyzer, Brookhaven model. Measurements were carried out using 1 ml of

$1 \times 10^{-4}$  Molar of sample in 10 ml buffer solution; in a quartz cuvette of zeta potential was measured at room temperature in different pH media.

The gravimetric analysis was carried out using Shimadzu thermogravimetric analyzer TGA-50. Measurements were carried out from ambient temperature to  $600\text{ }^\circ\text{C}$  at a heating rate of  $10\text{ }^\circ\text{C}/\text{min}$  in a nitrogen atmosphere at flow rate of  $20\text{ mL}/\text{min}$ . The morphology of the samples was examined using transmission electron microscope (TEM) JEOL: JEM-100cx).

### Preparation of magnetite nanoparticles

Super magnetic nanoparticles were prepared using chemical coprecipitation method (Jolivet et.al.2004). According to this method, 3.17 g of  $\text{FeCl}_2 \cdot 4\text{H}_2\text{O}$  (0.016 mol) and 7.57 g of  $\text{FeCl}_3 \cdot 6\text{H}_2\text{O}$  (0.028 mol) were dissolved in 320 mL of deionized water, such that  $\text{Fe}^{+2} / \text{Fe}^{+3} = 1 / 1.175$ . The mixture solution was stirred under nitrogen at  $80\text{ }^\circ\text{C}$  for one hour (Fig. 1A). Then 40 ml of  $\text{NH}_3 \cdot \text{H}_2\text{O}$  was injected into the mixture rapidly, stirred under nitrogen for another hour, and then cooled at room temperature (Fig.1B). The precipitated particles were washed five times with hot water, and ethanol and separated by magnetic decantation. Finally magnetic nanoparticles (Fig. 1C) were dried under vacuum at  $70\text{ }^\circ\text{C}$ . Consequently, the formation of  $\text{Fe}_3\text{O}_4$  nanoparticles occurred with black precipitation.

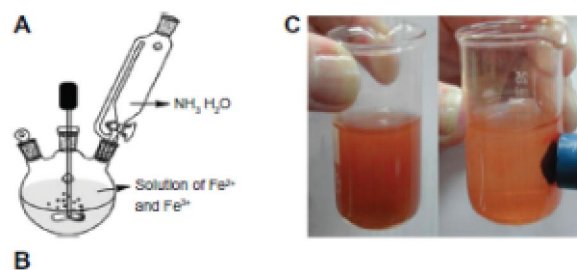


**Figure 1.** (A) Reactor of synthesis of supermagnetic magnetite nanoparticles, (B) preparation of nanoparticles, and (C) magnetite – ethanol suspension attached to a magnet.

### Magnetite nanoparticles coated by tris (hydroxymethyl) amino methane hydrochloride

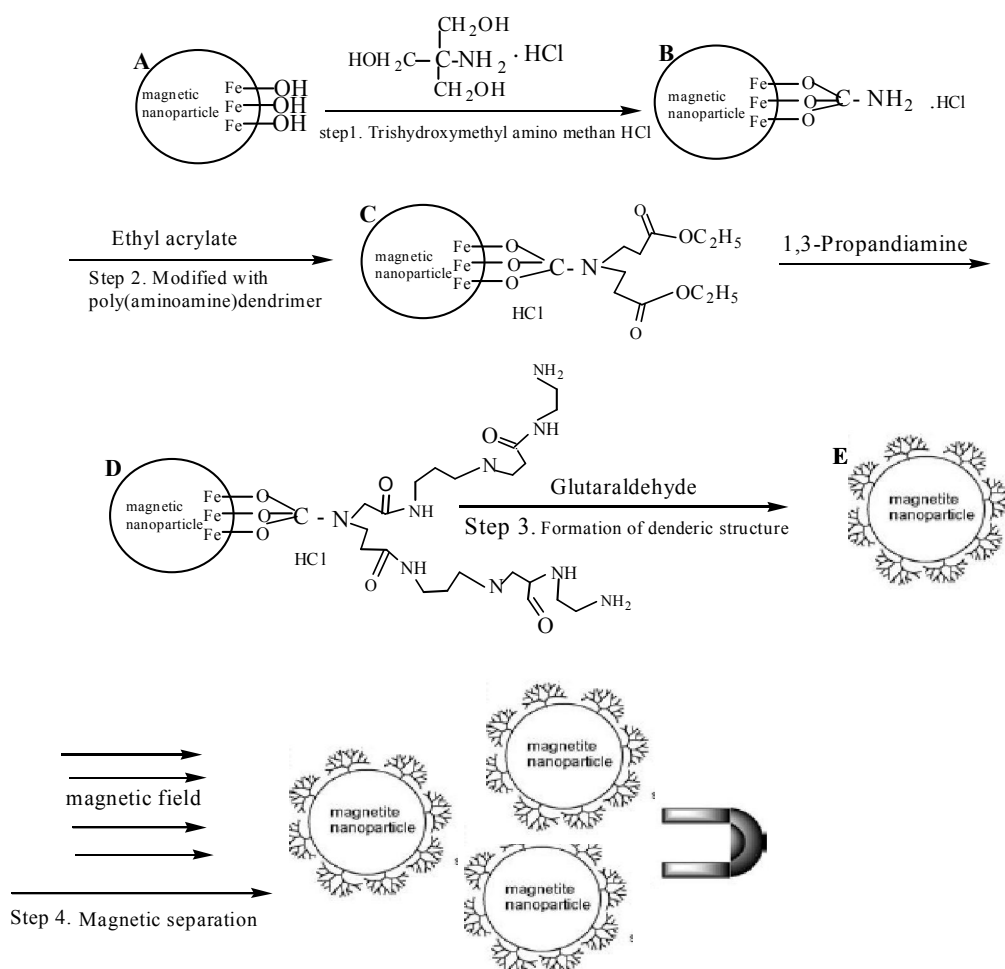
The 25 ml of magnetite colloid ethanol solution prepared above was diluted to 150 ml by ethanol. The solution was then treated by ultrasonic waves for 30 min. Then (0.075 g) of tris (hydroxymethyl) amino methane hydrochloride [ $\text{H}_2\text{N}-\text{C}-(\text{CH}_2\text{OH})_3 \cdot \text{HCl}$ ] in 25

ml ethanol by ratio (1:1) was added to the magnetite colloid solution with rapid stirring for 7 hours. The formed solution washed by methanol five times by magnetic separation. Tris (hydroxymethyl)amino methane hydrochloride-coated magnetite nanoparticles were dispersed in methanol. Thus,  $G_0$  represented the magnetite nanoparticles modified with tris (hydroxymethyl)amino methane hydrochloride.

#### Surface modification with PAMAM dendrimer

Dendrimer generation was initiated with 50 ml of  $G_0$  methanol solution. A 200 ml of ethyl acrylate 20% (v/v) in methanol solution was added and the suspension was immersed in an ultra sonicating water bath at room temperature for 7 hours. The particles were collected magnetically and rinsed with methanol

five times by magnetic separation. After rinsing, 40 ml of (v/v) of 1,3-propane diamine in methanol solution was added and the suspension was immersed in an ultra sonicating water bath at room temperature for 3 hours. The particles were rinsed with methanol five times by magnetic separation. Stepwise growth using ethyl acrylate and 1,3- propane diamine was repeated until the desired number of generation ( $G_0$ – $G_5$ ) was achieved (Scheme 1, Step 2, step 3). Finally the magnetic nanoparticles ( $G_0$ – $G_5$ ) was dispersed in 10 ml 5% glutaraldehyde aqueous solution with stirring for 3 hours at room temperature. The product was washed three times with 25 ml methanol and five times with 25 ml water by magnetic separation, finally dried in vacuum at 40 °C.



**Scheme 1.** Magnetite nanoparticle modified with PAMAM dendrimers( Bi - Feng et.al.2004).

#### Test microorganisms

Gram-Positive bacteria *staphylococcus auries*, Gram-negative bacteria *Escherichia coli* microorganism were isolated and supplied from bacteriology lab, microbiology research unit, Faculty of Science, Tanta University, Egypt. Agar disk

diffusion method was used for the determination of the preliminary pathogenic microorganisms.

#### Sample preparation for antimicrobial test by using cut pulg method for screening of antimicrobial activity

Cut plug method recorded by (Pridham et.al. 1956) was employed to determine the antimicrobial activity of the chosen products as follows: Freshly prepared spore suspension of different test microorganisms (0.5 ml of about  $10^6$  cells/ml) was mixed with 9.5ml of melting sterile Sabouraud's dextrose medium (for fungi) or nutrient agar medium (for bacteria) at 45 °C, poured on sterile Petri dishes, and left to solidify at room temperature. Regular wells were made in the inoculated agar plates by a sterile cork borer of 0.7 mm diameter. Each well was filled with 20 mg of each tested powder. Three replicas were made for each test, and all plates were incubated at 32 °C for 24 hours for bacteria. Then the average diameters of inhibition zones were recorded in centimeters, and compared for all plates.

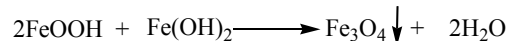
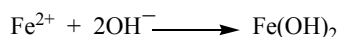
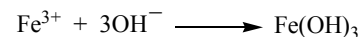
**MIC (minimal inhibitory concentration) determination for the most efficient antimicrobial compounds against test microorganisms**

Half-fold serial dilutions were made for selected **compounds** in order to prepare concentrations of 6.25, 12.5, 25, 50 and 100 mg/ml in distilled water, zero concentration was considered as a negative control. A previously prepared pure spore suspension of each test microorganism (0.5 ml of about  $10^6$  cells/ml) was mixed with 9.5 ml of each concentration in sterile test tubes, incubated at 27°C for 3 days for fungi, at 32°C for 24 hours for bacteria, then optical density of growth was measured by spectrophotometer (Optima SP-300, Japan) at 620 nm for each incubated mixture, results were represented graphically, and MIC was recorded for each tested material(Shadomy et.al. 1985 ).

### 3. Results and Discussion

#### Mechanism of $Fe_3O_4$ nanoparticles formation

During the precipitation of  $Fe_3O_4$  from  $Fe^{2+}$  and  $Fe^{3+}$  salts mixtures, two separate reactions could occur after addition of ammonium hydroxide to observe the precipitation of  $Fe_3O_4$  nanoparticles. It is well known that  $Fe(OH)_2$  and  $Fe(OH)_3$  formed at  $pH > 8$  by the hydroxylation of the ferrous and ferric ions under anaerobic condition. Consequently, the formation of  $Fe_3O_4$  nanoparticles occurred with black precipitation. The possible reaction for formation of  $Fe_3O_4$  nanoparticles as follow: the reaction is fast, very high yielding, and magnetite crystals are seen instantaneously after addition of the iron source. It is essential the whole reaction mixture be free of oxygen, otherwise magnetite can be oxidized to ferric hydroxide ( $\gamma - Fe_3O_4$ ) in the reaction mixture. The larger particles sizes can also be obtained by aggregation of small crystallites through synthesis (Sun et.al. 2006).



#### Optimized conditions for synthesis of $Fe_3O_4$ nanoparticles

##### FTIR – spectroscopy

In the present study FTIR spectra of the pristine tris (hydroxymethyl) amino methane hydrochloride (a),  $Fe_3O_4$  nanoparticles (b), and PAMAM dendrimer – modified iron oxide nanoparticles (c) are shown in Table 1 and Fig. 2. For both samples (b) and (c), the analysis indicated absorption peaks at 440, 530, 620, and 3402  $cm^{-1}$  corresponding to the Fe-O vibration bonds related to the magnetite phase(Mahdavi et.al.2013).

**Table 1. Fourier transform infrared spectrum for  $Fe_3O_4$**

System	Infrared bands ( $cm^{-1}$ )	Descriptions
	440	Absorption band of Fe-O
	580	Absorption band of Fe-O
$Fe_3O_4$	620	Absorption band of Fe-O
	3042	OH vibrations

As shown in Fig. 2, the PAMAM dendrimer-coated iron oxide exhibited the absorption bands of C-H stretch (at 3010 and 2955  $cm^{-1}$ ), bending vibration of  $-NH_2$  group (at 3285  $cm^{-1}$ ),  $-CO-NH-$  group (at 1650, 1555, and 1462  $cm^{-1}$ ), in addition to the characteristic absorption of the Fe-O of magnetite at 579  $cm^{-1}$  (Shen et.al. 2009). All of these reveal the existence of PAMAM dendrimer. In curve (a), absorption band at 2854  $cm^{-1}$  was attributed to the symmetric  $CH_2$  stretching. The intense peak at 3010  $cm^{-1}$  shifted to 3116  $cm^{-1}$  concerned to amino group. The tertiary hydroxyl groups were found between 1200–1150  $cm^{-1}$  and the band of amino group was appeared at 3300  $cm^{-1}$ .

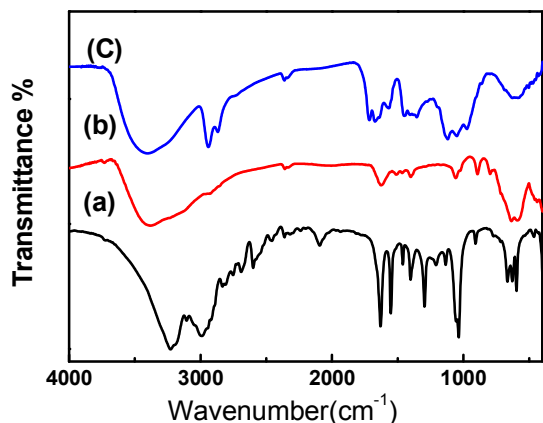


**Figure 2.** FT-IR spectra of (a) tris(hydroxymethyl) amino methane hydrochloride, (b) pure  $\text{Fe}_3\text{O}_4$  nanoparticles, and (c) PAMAM dendrimer-coated iron oxide.

#### XRD-diffraction spectroscopy

The XRD patterns of the pristine  $\text{Fe}_3\text{O}_4$  (a) and PAMAM dendrimer-coated iron oxide (b) in Fig.3. A series of characteristic peaks were observed in the XRD pattern at  $2\theta$  of  $9.6^\circ$ ,  $30.1^\circ$ ,  $35.5^\circ$ ,  $43.1^\circ$ ,  $54.5^\circ$ ,  $57.6^\circ$ , and  $63.6^\circ$  corresponding to the diffractions to the diffractions of  $220^\circ$ ,  $311^\circ$ ,  $400^\circ$ ,  $422^\circ$ ,  $511^\circ$  and  $440^\circ$  crystal faces of  $\text{Fe}_3\text{O}_4$  spinel structure. The positions and relative intensities of the reflection peak of  $\text{Fe}_3\text{O}_4$  nanoparticles agree with the XRD diffraction peaks of standard  $\text{Fe}_3\text{O}_4$  samples (Thunemann et.al. 2006). Indicating that the black-colored magnetic powders are magnetite nanoparticles. Sharp peaks also suggest that the  $\text{Fe}_3\text{O}_4$  nanoparticles have good crystallize structure. Peak broadening observed is consistent with the small particle size (Esquivelet.al. 2007). It was found that the magnetite crystallites could be well indexed to the inverse cubic spinel structure of  $\text{Fe}_3\text{O}_4$ . The XRD data further suggest that the effect of the poly amino amine [PAMAM dendrimer-coated iron oxide] on the crystal structure sample is negligible.

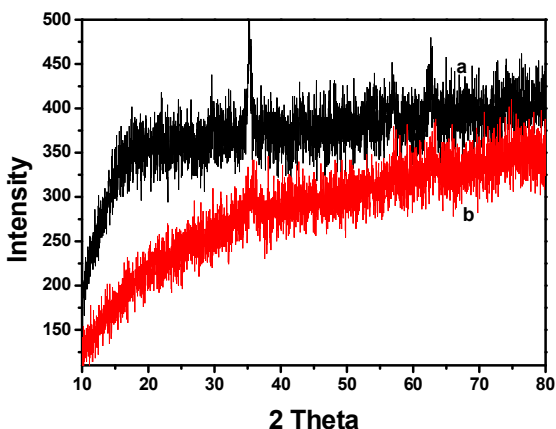


**Figure 3.** XRD patterns of (a)  $\text{Fe}_3\text{O}_4$ , and (b) and PAMAM dendrimer-coated iron oxide.

#### Thermo gravimetric analysis (TGA)

The indication of the coating formation in the magnetite nanoparticle surface can be obtained from TGA measurement. Fig 4 showed the typical TGA / DTA curves of dry magnetite nanoparticles modified PAMAM dendrimer-coated iron oxide. There are fifth derivative peaks in the DTA curve which related to the mass losses in the TGA curve. The first peak is at about  $135^\circ\text{C}$ , the weight loss is due to dehydration process of the water contained in the poly amino amine [PAMAM dendrimer-coated iron oxide], and the percentage of mass loss is 7% can be attributed to the loss of water associated with the magnetite dendrimer. At the second step from  $135^\circ\text{C}$  to  $242^\circ\text{C}$ , which is around the decomposition of the poly amino amine [PAMAM dendrimer-coated iron oxide] due to intermolecular dehydration and anhydration formation on the dendrimer. The third step of the thermal degradation at  $290^\circ\text{C}$  the weight loss can be explained by the fact that the dendrimer molecules loss  $\text{NH}_2$  and  $\text{CO}_2$  from its skeleton structure. The fourth stage at  $380^\circ\text{C}$  –  $490^\circ\text{C}$ , and the percentage of mass loss is about 63% which is attributed to the phase transition from  $\text{Fe}_3\text{O}_4$  to  $\text{FeO}$ . The fifth derivatives at  $450^\circ\text{C}$ – $600^\circ\text{C}$ , related to a percentage mass loss of 42%, possibly because of the deoxidation of Fe-O is thermodynamically stable above  $570^\circ\text{C}$  in phase diagram of the Fe-O system. Since the TGA/DTA analysis was achieved under the  $\text{N}_2$  atmosphere (Zhao et.al.2006).

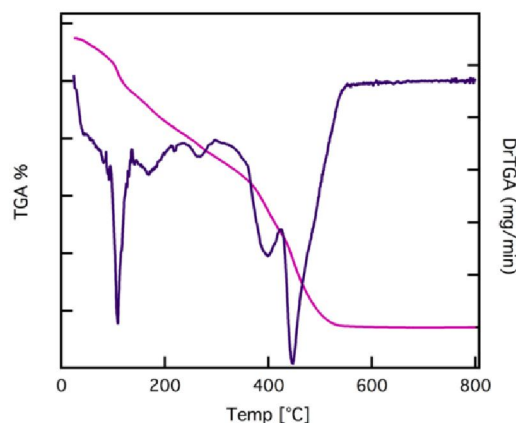


**Figure 4.** TGA/DTGA curves of PAMAM dendrimer-coated iron oxide.

#### UV-Vis absorption measurements

The absorption spectrum of  $\text{Fe}_3\text{O}_4$  nanoparticles showed a broad absorption band in the range of 250–600 nm which due to charge transfer spectra (Hussain et.al. 2003) (Fig. 5). When turning to PAMAM

dendrimer-coated iron oxide, the absorption spectrum exhibited increase in the absorption intensity in the range of 250-600 nm and reaches its maximum at around 231 nm.

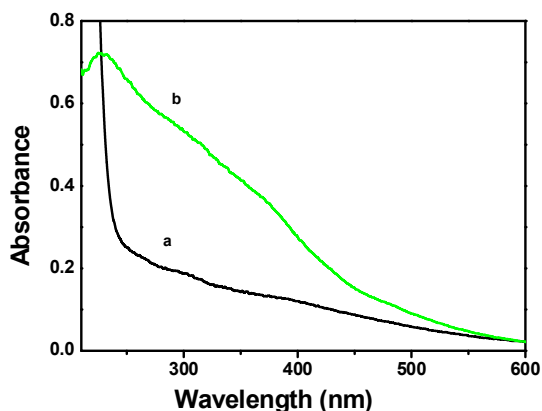


**Figure 5.** UV-Vis absorption spectra of  $\text{Fe}_3\text{O}_4$  (a) and PAMAM dendrimer-coated iron oxide (b).

### Zeta potential

Zeta potential technique is used a measure of the magnitude of the electrostatic or charge repulsion/attraction between particles, and is one of the fundamental parameters known to affect stability. The magnitude of the zeta potential indicates the degree of electrostatic repulsion between adjacent, similarly charged particles in a dispersion (Hanaor et.al. 2012; Greenwood and Kendall 1999).

A plot of zeta potential of PAMAM dendrimer coated- $\text{Fe}_3\text{O}_4$  nanoparticles versus pH (2.0–8.2) are shown in Fig. 6. The dendrimer which terminated by  $\text{NH}_2$  groups exhibited positive zeta potential at low pH. However, here it decreased with increasing pH and became zero at pH about 4.5. This may be due to the presence of a Stern layer formed by negatively charged and neutralized the positive surface. Isoelectric point decrease after the dendrimerization of

magnetite nanoparticle and reaches relative stable value of about pH (6.2 – 7.2) for magnetite nanoparticles due to the positive charge of  $-\text{NH}_3$  on the magnetite surface (Sudhanshu et.al. 2012).

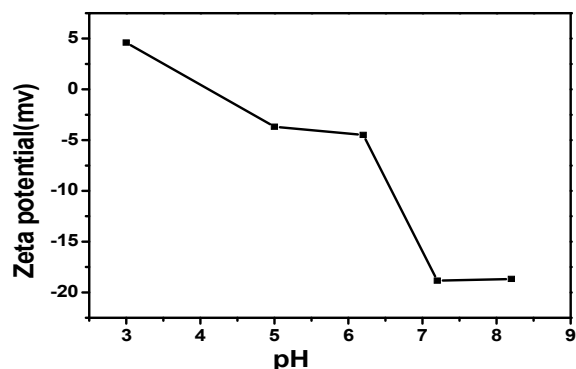


**Figure 6.** Zeta potential of PAMAM dendrimer coated- $\text{Fe}_3\text{O}_4$  nanoparticles at different pH values.

### Transmission electron microscopy (TEM)

Fig. 7 shows TEM images and size distribution of pristine (a)  $\text{Fe}_3\text{O}_4$  nanoparticles and (b) PAMAM dendrimer-coated iron oxide nanoparticles. It can be seen that the pristine  $\text{Fe}_3\text{O}_4$  nanoparticles were polydisperse and seriously aggregated. After surface modification by the PAMAM dendrimer the particles maintained their original shape with a good monodispersity. The particle size is very uniform with the average size of about 7.4 nm for  $\text{Fe}_3\text{O}_4$  nanoparticles. The average particle size of the PAMAM dendrimer-coated iron oxide was about 6.3 nm which is lower than the  $\text{Fe}_3\text{O}_4$  nanoparticles. From the magnified image a slight aggregation can be observed which was due to the aggregation of individual particles with an incomplete coating by the PAMAM dendrimer.

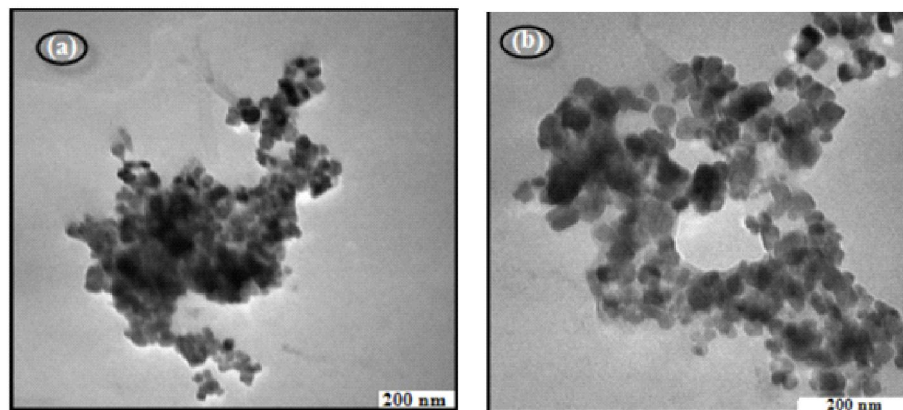


**Figure 7.** TEM images (a) Fe<sub>3</sub>O<sub>4</sub> nanoparticles and (b) PAMAM dendrimer-coated iron oxide nanoparticles at direct magnification 50000X.

#### Antimicrobial Test

#### Antimicrobial Activity of Fe<sub>3</sub>O<sub>4</sub> nanoparticles and dendrimer PAMAM-coated Fe<sub>3</sub>O<sub>4</sub> nanoparticles

Antibacterial activities of Fe<sub>3</sub>O<sub>4</sub> nanoparticles and PAMAM dendrimer-coated Fe<sub>3</sub>O<sub>4</sub> nanoparticles

against Gram-negative and Gram-positive bacteria considered in the present study were qualitatively and quantitatively assessed by determining/observing the presence of inhibition zones and MIC values.

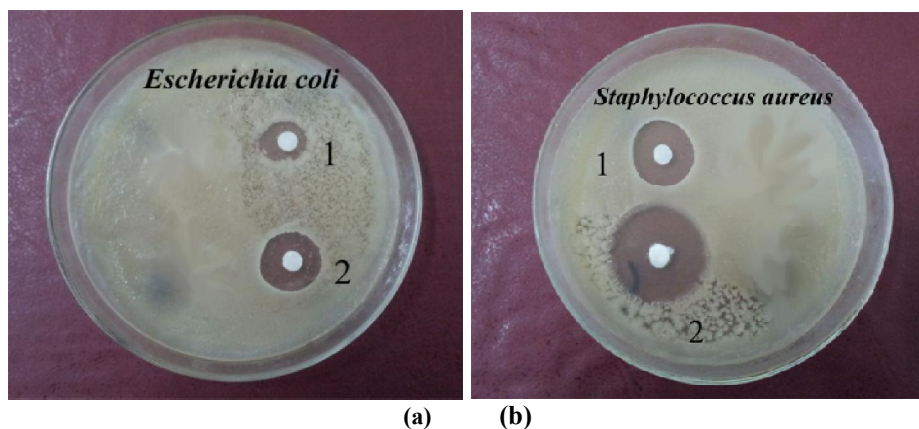


**Figure 8.** Antimicrobial activity of Fe<sub>3</sub>O<sub>4</sub> nanoparticles and dendrimer PAMA-coated Fe<sub>3</sub>O<sub>4</sub> nanoparticles against *E. coli* bacteria (a) and *Staphylococcus aureus* (b).

As can be observed from the inhibition zones of the PAMAM dendrimer-coated Fe<sub>3</sub>O<sub>4</sub> nanoparticles were higher than Fe<sub>3</sub>O<sub>4</sub> nanoparticles as shown in Table 2.

**Table 2. Inhibition zones of different sensitive microorganisms**

Test Material	<i>Escherichia coli</i>	<i>Staphylococcus aureus</i>
<b>a</b>	1.4nm	1.3nm
<b>b</b>	1.8nm	1.9nm

The antibacterial activities of the Fe<sub>3</sub>O<sub>4</sub> nanoparticles (a), the dendrimer-coated Fe<sub>3</sub>O<sub>4</sub> nanoparticles (b) against two pathogenic bacteria (+ve) gram *Staphylococcus aureus* and (-ve) gram *Escherichia coli* are represented in Table 2 and Fig. 8. The result of antibacterial activity showed moderate antibacterial activity against *Escherichia coli* with inhibition zone 1.4 nm for Fe<sub>3</sub>O<sub>4</sub> nanoparticles (a) & 1.8 nm for the dendrimer-coated Fe<sub>3</sub>O<sub>4</sub> nanoparticles (b), while the antibacterial activity against *Staphylococcus aureus* with inhibition zone detected 1.3 nm for Fe<sub>3</sub>O<sub>4</sub> nanoparticles (a) & 1.9 nm for the dendrimer-coated Fe<sub>3</sub>O<sub>4</sub> nanoparticles (b) showed in Table 2.

The main mechanism by which particles showed antibacterial might be via oxidative stress generated by ROS (Mahdy et.al. 2012; Tran et.al. 2010). ROS, including superoxide radicals (O<sup>2-</sup>), hydroxyl radicals (

OH), hydrogen peroxide (H<sub>2</sub>O<sub>2</sub>), and singlet oxygen (<sup>1</sup>O<sub>2</sub>), can cause damage to protein and DNA in bacteria. In the present study, metal oxide (FeO) in both nanoparticles (a) & (b) could be the source that created ROS leading to the inhibition of most pathogenic bacteria including *Staphylococcus aureus*.

A similar process was also described by (Kim et.al. 2007) in which Fe<sup>2+</sup> reacted with oxygen to create hydrogen peroxide (H<sub>2</sub>O<sub>2</sub>). This H<sub>2</sub>O<sub>2</sub> consequently reacted with ferrous ions via the Fenton reaction and produced hydroxyl radicals which are known to damage biological macromolecules (Touati 2000).

(Lee et.al.2008), reported that the inactivation of *E. Coli* by zero-valent iron nanoparticles could be because of penetration of the small particles size into *E. Coli* membranes. It also important to note that iron oxide nanoparticles do not negatively influence all cells and thus it can be said that an appropriate external magnetic field be directed to kill bacteria as needed throughout the body.

The determination of (MIC) is the minimal inhibitory concentration of the surviving cell number % is defined as the lowest concentration of the antimicrobial that will inhibit the visible growth of microorganisms after overnight incubation was tabulated in Table 3 for the dendrimers-coated Fe<sub>3</sub>O<sub>4</sub>nanoparticle (b) and represented in Fig. 9.

To investigate the minimum volume of nanoparticles needed for the onset of bacteria inhibition, minimum inhibitory concentration tests

were performed while monitoring growth characteristics of the (+ve) Gram *Staphylococcus aureus*, (-ve) Gram *Escherichia coli* bacteria (Fig. 9)

for the PAMAM dendrimer-coated  $\text{Fe}_3\text{O}_4$  nanoparticles at five concentrations, 0  $\mu\text{M}$  to 100  $\mu\text{M}$ .

**Table 3. MIC of selected chemical compounds against different sensitive microorganisms**

Sample	Percentage of surviving cells (% Optical density)						Microorganism
	Concentration (mg/ml)						
	0.0	6.25	12.5	25	50	100	
B	100	72	58	27	28	26	<i>Escherichia coli</i>
	100	81	53	31	30	32	<i>Staphylococcus aureus</i>

From the results of the MIC test, the minimum volume of dendrimer-coated  $\text{Fe}_3\text{O}_4$  nanoparticles necessary to exhibit antimicrobial activity against (+ve) gram & (-ve) gram bacteria. That is, at volumes below this critical value, no prevention of bacterial growth was observed when tested against the *Staphylococcus aureus* bacteria. As the volume of the nanoparticle solution increased, the absorbance decreased dramatically. This clearly indicates that larger amounts of bacteria have been killed.

Comparatively, for the higher concentrated dendrimer-coated  $\text{Fe}_3\text{O}_4$  nanoparticles a lower absorbance is observed when tested against the *E. coli* bacteria than *Staphylococcus aureus*. In other words, this is a direct indication that the dendrimer-coated  $\text{Fe}_3\text{O}_4$  nanoparticles performed better at killing the bacteria at higher concentrations. These results further support the observation that the dendrimer-mediated growth the antimicrobial activity is still observed against both Gram-negative and Gram-positive bacteria.

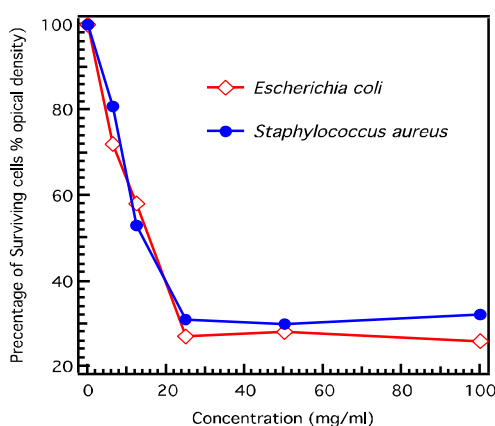


**Figure 9.** MIC test revealing the minimum volume of dendrimer-coated  $\text{Fe}_3\text{O}_4$  nanoparticles (b) needed to exhibit antimicrobial activity against *E. coli* & *Staphylococcus aureus* bacteria

The mode action of (the dendrimer-coated  $\text{Fe}_3\text{O}_4$  nanoparticles) bioactive materials were interpreted in terms of the following sequence process (Kanazawa

et.al. 1993 ): (1) adsorption onto the bacterial cell surface, (2) diffusion through the cell wall, (3) binding to the cytoplasmic membrane, and (4) release of cytoplasmic constituent such as  $\text{K}^+$  ion, DNA, and RNA, and death of the cell. Therefore the adsorption of Gram (+ve) *Staphylococcus aureus* bacterial cell surfaces expected to be enhanced than gram (-ve) *E. coli*.

### Conclusions

In this research study, we present the successful synthesis of superparamagnetic  $\text{Fe}_3\text{O}_4$  nanoparticles and the dendrimer-coated  $\text{Fe}_3\text{O}_4$  nanoparticles with an average diameter around 6.3–7.4 nm. Physical characteristics of the PAMAM dendrimer-coated  $\text{Fe}_3\text{O}_4$  nanocomposite were studied using (IR), TEM, UV-Vis, X-ray, TGA, zeta potential and TEM images. In general, PAMAM dendrimer-coated  $\text{Fe}_3\text{O}_4$  nanoparticles showed good antimicrobial activity against the tested microorganism. TEM analyses revealed that the nanoparticles exhibited a single-phased, spherical in shape, and monodispersed in nature. PAMAM dendrimer-coated  $\text{Fe}_3\text{O}_4$  nanoparticles and  $\text{Fe}_3\text{O}_4$  nanoparticles exhibited antibacterial activities against both Gram-Positive bacteria *staphylococcus aureus*, Gram-negative bacteria *Escherichia coli* microorganism. The activities were more pronounced in the Gram-positive bacteria as compared to the Gram-negative bacteria. In addition, paper disk diffusion assay tests revealed higher zones of inhibition for the dendrimer-coated  $\text{Fe}_3\text{O}_4$  nanoparticles using (+ve) Gram bacteria than (-ve) Gram bacteria. MIC test revealed that the minimum volume (i.e., critical inhibiting volume) needed to initiate the onset growth prevention of bacteria. No antimicrobial activity was observed for the low in concentration dendrimers. This could begin to unlock the unlimited possibilities of applications of dendrimer-coated  $\text{Fe}_3\text{O}_4$  nanoparticles to the future of research in biomedicine and the production of pharmaceuticals.

### References

1. Bi - Feng P, Feng G, Hong - Chen G 2004.

2. Dendrimer modified magnetite nanoparticles for protein immobilization. *J. Colloid and Interface Science*; 284: 1 – 6.
3. Chan HT, DO YY, Huang PL, Chien PL, Chan TS 2006. Preparation and properties of biocompatible magnetic Fe<sub>3</sub>O<sub>4</sub> nanoparticles. *J. Magn Magn. Mater.*304: 415 - 417.
4. Duncan R, Izzo L 2005. Dendrimer biocompatibility and toxicity. *Adv. Drug Deliv. Rev.* 57(15): 2215 – 2237.
5. E.I-Khouly ME, Kang ES, Kay KY, Choi CS, Araki Y, Ito OA 2008. New Blue-Light Emitting Polymer: Synthesis and Photoinduced Electron Transfer Process. *J. Polymer Sci.: Part A: Polymer Chem.* 46(12): 4249 - 4253.
6. El-Khouly ME., Chen Y, Zhuang X, Fukuzumi S 2009. Long-Lived Charge-Separated Configuration of a Push-Pull Archetype of Disperse Red 1 End-Capped Poly[9,9-Bis(4-diphenylaminophenyl)fluorene]. *J. Am. Chem. Soc.: Part A: Polymer Chem.* 131(18): 6370 - 6371.
7. Esquivel J, Facundo IA, Trevino ME, Lopez RG 2007. A novel method to prepare magnetic nanoparticles: precipitation in bicontinuous microemulsions. *J. Mater. Sci.* 42: 9015- 9020.
8. Gao BF, Zhen MW, Ao LM, Gu HC 2005. Study of streptavidin coated onto PAMAM dendrimer modified magnetite nanoparticles. *J. Magn Magn Mater.*293: 293, 48-54.
9. Gupta AK, Gupta M 2005. Synthesis and surface engineering of iron oxide nanoparticles for biomedical application. *Biomaterials.* 26(18): 3395 - 4021.
10. Greenwood R, Kendall K 1999. Selection of suitable dispersants for aqueous suspensions of Zirconia and Titania powders using acoustophoresis. *J. Eur. Ceramic Soc.* 19(4):479 – 488.
11. Huh YM, Jun YM, Song HT, Kim S, Choi JS, Lee JH 2005. In vivo magnetic resonance detection of cancer by using multifunctional magnetic nanocrystals. *J. Am. Chem. Soc.* 127: 12387 – 12391.
12. Hussain N, Singh B, Sakthivel T, Florence AT 2003. Corrigendum to Formulation and stability of surface-tethered DNA-gold – dendron nanoparticle. *Int. J. Pharm.* 54: 27- 31.
13. Hanaor DAH, Michelazzi M, Leonelli C, Sorrell CC 2012. The effects of carboxylic acids on the aqueous dispersion and electrophoretic deposition of ZrO<sub>2</sub>. *J. Eur. Ceramic Soc.* 32(1): 235- 244.
14. Ito A, Kuga Y, Honda H, Kikkawa H, Horiuchi A, Watanabe Y 2004. Magnetite nanoparticle-loaded anti-HER2 immunoliposomes for combination of antibody therapy with hyperthermia. *Cancer Lett.* 212(2): 167 – 175.
15. Jain TK, Morales MA, Sahoo SK, Leslie-Pelecky DL, Labhasetwar V 2005. Iron oxide nanoparticles for sustained delivery of anticancer agents. *Mol. Pharm.* 2: 194 – 205.
16. Jolivet JP, Chnane'ac C, Tronc E 2004. Iron oxide chemistry. From molecular clusters to extended solid networks. *Chem. Commun.* 4(5): 481 – 487.
17. Kim YH, Lee DK, Cha HG, Kim CW, Kang YS 2007. Synthesis and characterization of antibacterial Ag-SiO<sub>2</sub> nanocomposite. *J. Phys. Chem.* 11: 3629 – 3635.
18. Kim JS, Kuk E, Yu KN 2007. Antimicrobial effects of silver nanoparticles. *Nanomedicine: Nanotechnology Biology and Medicine.* 3(1): 95 -101.
19. Lee C, Kim JW, Lee WI, Nelson KL, Yoon, J 2008. Bacterial effect of zero-valent iron nanoparticles on Escherichia coli. *Environmental Science & Technology.* 42(13): 4927 – 4933.
20. Mornet S, Vasseur S, Garraset F, Duguet E 2004. Magnetic nanoparticle design for medical diagnosis and therapy. *J. Mater Chem.*14: 2161 - 2175.
21. Mornet S, Portier J, Duguet E 2005. A method for synthesis and functionalization of ultrasmall superparamagnetic covalent carriers based on maghemite and dextran. *J. Magn Magn Mater.* 293: 127 – 134.
22. Mahdavi M, Ahmed MB, Haron MJ, Gharayebi Y 2013. Fabrication and characterization of SiO<sub>2</sub> \ (3- aminopropyl)triethoxysilane – coated magnetite nanoparticles for lead (II) removal from aqueous solution. *J. Inorg. Organomet. Polym.* 23: 599 - 607.
23. Mahdy SA, Raheed QJ, Kalaichelvan PT 2012. Antimicrobial activity of zero-valent iron nanoparticles. *International Journal of Modern Engineering Research.* 2(1): 578- 581.
24. Pankhurst QA, Thanh NKT, Jones SK, Dobson J 2009. Progress in application of magnetic nanoparticles in biomedicine. *J. Physics D.* 42: 224 – 243.
25. Pridham T, Lindenfesler L, Shotwell O, Stodola F, Benedict R, Foley C J. 1956 Antibiotics against plant diseases: A laboratory and green house survey. *Phytopathology.*46: 568 - 575.
26. Severson S, Tomalia DA 2005. Dendrimers in biomedical application – reflections on the field. *Adv. Drug. Deliv. Rev.*57: 2106 – 2129.
27. Shadomy S, Epsinel I, Cartwright R 1985: Laboratory studies agents: Susceptibility test and bioassays. In: Lennette A, Balows W, Hausler H,

- and Shadomy S 4<sup>th</sup> ed. of: Manual of Clinical Microbiology, Little Brown Co., Boston.
28. Sun J, Zhou S, Hou P, Yang Y, Weng J, Weng X 2006. Synthesis and characterization of biocompatible Fe<sub>3</sub>O<sub>4</sub> nanoparticles. *J. Biomed. Mater. Res. Part A*. 10: 333- 341.
  29. Shen YF, Tang J, Nie ZH, Wang YD, Ren Y 2009. Preparation and application of magnetic Fe<sub>3</sub>O<sub>4</sub> nanoparticles for wastewater purification. *Sep. Purif. Technol.* 68: 312 – 319.
  30. Sudhanshu SB, Jayanta KP, Krishna P, Niladri P, Hrudayanath T 2012. Characterization and Evaluation of Antibacterial Activities of Chemically Synthesized Iron Oxide Nanoparticles. *World Journal of Nano Science and Engineering*. 2: 196 - 200.
  31. TomaliaDA, Naylor AM., Goddard WA 1990. Starburst dendrimers molecular – level control of size, shape, surface chemistry, topology, and flexibility from atoms to macromolecules. *Angew. Chem. Int. Ed. Engl.*, 29: 138 – 175.
  32. Theivasanthi T, Alagar M 2011. Studies of Copper Nanoparticles Effects on Microorganisms. *Annals of Biological Research*. 2: 368 – 373.
  33. Thunemann AF, Schutt D, Kaufner L, Pison U, Mohwald H 2006. Maghemite nanoparticles protectively coated with poly(ethyleneimine) and poly(ethylene oxide)- blockpoly (glutamic acid). *Langmuir*. 22: 2351 - 2357.
  34. Tran N, Mir A, Mallik D, Sinha A, Nayar S, Webster TJ 2010. Bactericidal effect of iron oxide nanoparticles on *Staphylococcus aureus* International of *Nanomedicine*. 5(1): 277 – 283.
  35. Touati D 2000. Iron and oxidative stress in bacteria. *Archives of Biochemistry and Biophysics*. 237(6): 1 – 6.
  36. Zhao SY, Lee DK, Kim CW, Cha HG, Kim YH 2006. Synthesis of magnetic nanoparticles of Fe<sub>3</sub>O<sub>4</sub> and Co-Fe<sub>2</sub>O<sub>3</sub> and their surface modification by surfactant adsorption. *Bull Korean Chem. Soc.* 27: 237- 242.
  37. Zawa A, Ikeda T, Endo T 1993. Novel polycationic biocides: Synthesis and antibacterial activity of polymeric phosphonium salts. *J. Polym. Sci.: Part A Polymer Chemistry*. 31(2): 335 – 343.

6/21/2015